APL Photonics

Invited Article: Mitigation of dynamical instabilities in laser arrays via non-Hermitian coupling

Cite as: APL Photonics 3, 060802 (2018); https://doi.org/10.1063/1.5028453
Submitted: 10 March 2018 . Accepted: 19 April 2018 . Published Online: 01 June 2018

S. Longhi, and L. Feng

Invited Article: Mitigation of dynamical instabilities in laser arrays via non-Hermitian coupling

S. Longhi[1,a)] and L. Feng[2]
[1]*Dipartimento di Fisica, Politecnico di Milano and Istituto di Fotonica e Nanotecnologie del Consiglio Nazionale delle Ricerche, Piazza L. da Vinci 32, I-20133 Milano, Italy*
[2]*Department of Materials Science and Engineering, University of Pennsylvania, Philadelphia, Pennsylvania 19104, USA*

(Received 10 March 2018; accepted 19 April 2018; published online 1 June 2018)

Arrays of coupled semiconductor lasers are systems possessing complex dynamical behavior and are of major interest in photonics and laser science. Dynamical instabilities, arising from supermode competition and slow carrier dynamics, are known to prevent stable phase locking in a wide range of parameter space, requiring special methods to realize stable laser operation. Inspired by recent concepts of parity-time ($\mathcal{PT}$) and non-Hermitian photonics, in this work, we consider non-Hermitian coupling engineering in laser arrays in a ring geometry and show, both analytically and numerically, that non-Hermitian coupling can help to mitigate the onset of dynamical laser instabilities. In particular, we consider in detail two kinds of nearest-neighbor non-Hermitian couplings: symmetric but complex mode coupling (type-I non-Hermitian coupling) and asymmetric mode coupling (type-II non-Hermitian coupling). Suppression of dynamical instabilities can be realized in both coupling schemes, resulting in stable phase-locking laser emission with the lasers emitting in phase (for type-I coupling) or with $\pi/2$ phase gradient (for type-II coupling), resulting in a vortex far-field beam. In type-II non-Hermitian coupling, chirality induced by asymmetric mode coupling enables laser phase locking even in the presence of moderate disorder in the resonance frequencies of the lasers. https://doi.org/10.1063/1.5028453

I. INTRODUCTION

Non-Hermitian and parity-time ($\mathcal{PT}$) symmetric photonics, i.e., the ability of molding the flow of light in synthetic optical media by judicious spatial distribution of optical gain and loss, is an emerging and active area of research in optics (see, e.g., Refs. 1–5 and references therein). Inspired by concepts of non-Hermitian quantum mechanics[6–9] and originally conceived to provide an experimentally accessible testbed to emulate in optics non-Hermitian scattering potentials and quantum phase transitions,[10–18] $\mathcal{PT}$ symmetric photonics has demonstrated to be a fertile and technologically accessible research field which is promising for a wealth of interesting applications[19–50] ranging from material transparency and invisibility,[22–26] laser-absorber devices,[19,20,30,34] microlaser engineering and mode selection,[27–29,31,33,37,39] polarization mode conversion,[40] light structuring and transport,[32,35] optical sensing,[41–44] topological lasers,[47–49] etc. The application of the concepts of non-Hermitian optics in integrated laser devices, i.e., beyond linear models, meets the problem of complexity and nonlinear instabilities typical of laser systems.[51–53] $\mathcal{PT}$ symmetry and non-Hermitian engineering have recently emerged as useful tools in the control of laser dynamics,[27–29,31–33,37–39,45,46,48,49] including systems of coupled laser arrays,[38,45–48] and in laser mode locking.[54]

Stable oscillation of arrays of coupled lasers in a given supermode is a longstanding problem in laser science and technology.[55–79] Avoiding instabilities is of great technological importance for the

a)Electronic mail: longhi@fisi.polimi.it

realization of high-power laser arrays and for a variety of applications in optical communications, sensing, and imaging.[55–58] Unfortunately, stable phase-locked oscillation in laser arrays is often prevented by supermode competition and laser instabilities:[60,63,66,67,69–71,74,77,79] the complicated array dynamics can lead to unstable behavior in a wide range of physically meaningful parameter space. Careful laser design, based on gain tailoring and/or special diffractive coupling, is hence needed to achieve stable phase locking operation.[59,61,62,64,65,68,75,76] In particular, in semiconductor lasers, the slow carrier dynamics and the large linewidth enhancement factor severely narrow the parameter space region of stable phase locking laser operation.

In this article, we apply concepts of non-Hermitian photonics to the control of the dynamical behavior of coupled semiconductor lasers in a ring geometry and show both analytically and numerically that nearest-neighbor non-Hermitian coupling engineering can help in suppressing the onset of dynamical instabilities. In particular, we consider in detail two kinds of nearest-neighbor non-Hermitian couplings, the so-called type-I and type-II non-Hermitian couplings. We show that suppression of dynamical instability can be realized, resulting in stable phase-locking laser emission with the lasers emitting with the same phase (for type-I non-Hermitian coupling) or with $\pi/2$ phase slip one another (for type-II non-Hermitian coupling). In the latter case, a vortex far-field beam can be achieved. The paper is organized as follows. Section II describes the rate equation model for coupled semiconductor lasers in a ring geometry and with rather general global or local (nearest-neighbor) non-Hermitian coupling and presents simple phase-locked stationary states under a few coupling schemes. The stability analysis of the phase-locked solutions is presented in Sec. III, where analytical stability boundaries are derived using an asymptotic method. In particular, it is shown that appropriate tailoring of non-Hermitian neighboring couplings can lead to suppression of dynamical (Hopf) instability generally observed when dealing with Hermitian coupling.[69] In Sec. IV, some numerical results are presented, which confirm the predictions of the theoretical analysis. Finally, the main conclusions are summarized in Sec. V.

II. SEMICONDUCTOR LASER ARRAYS WITH NON-HERMITIAN COUPLING

A. Rate equation model

We consider an array of N semiconductor lasers in a ring geometry,[66,69,78,80–82] schematically depicted in Fig. 1(a), which are locally or globally coupled by either evanescent mode coupling or

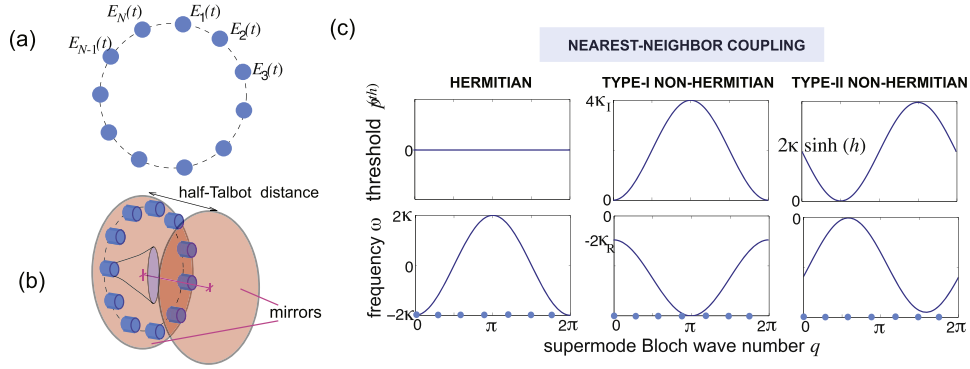

FIG. 1. (a) Schematic of an array made of N coupled semiconductor lasers on a ring. The coupling can be either local, throughout evanescent mode coupling (nearest-neighbor coupling), or global via some external cavity [for example diffractive coupling in a Talbot cavity, as shown in panel (b)]. Discrete rotational invariance along the ring is assumed. This means that the matrix of coupling constants $\kappa_{n,l}$ is a function of index difference $(l-n)$ solely, i.e., $\kappa_{n,l} = \kappa_{l-n}$. Dissipative coupling makes the coupling matrix non-Hermitian. (c) Typical behavior of normalized excess pump current threshold $p^{(th)}$ and oscillation frequency ω of stationary array supermodes versus Bloch wave number q for three kinds of nearest-neighbor couplings: Hermitian coupling $\kappa_{-1} = \kappa_1 = \kappa$, with κ real positive (left panels); type-I non-Hermitian coupling $\kappa_{-1} = \kappa_1 = \kappa_R + i\kappa_I$, with κ_R, κ_I real and positive (central panels); type-II non-Hermitian coupling $\kappa_{-1} = \kappa \exp(-h)$, $\kappa_1 = \kappa \exp(h)$ with κ, h real and positive (right panels). The Bloch wave number q of supermodes is quantized according to Eq. (11) given in the text and can assume N values.

by some diffractive coupling technique (see, for instance, Refs. 56, 59, 62, 64, 65, 68, 73, 75, 76, 78, and 80–82 and references therein). The rate equations that describe the temporal evolution of the slowly varying complex amplitudes of normalized electric fields E_n and normalized excess carrier density Z_n in each laser read as[63,67,69,77]

$$\frac{dE_n}{dt} = (1 - i\alpha)Z_n E_n - i\sum_{l=1}^{N} \kappa_{n,l} E_l, \tag{1}$$

$$T\frac{dZ_n}{dt} = p - Z_n - (1 + 2Z_n)|E_n|^2 \tag{2}$$

($n = 1, 2, \ldots, N$), where t is the dimensionless time in units of the photon lifetime τ_p, α is the linewidth-enhancement factor (typically $\alpha \simeq 3$–5), p is the normalized excess pump current, $T = \tau_s/\tau_p$ is the ratio between the spontaneous carrier lifetime τ_s and the photon lifetime τ_p (typically in the range $T \sim 100$–1000), and the matrix $\kappa_{n,l}$ describes the coupling between the various lasers in the array. As in Refs. 67 and 69, in writing Eqs. (1) and (2), we neglected time-delay effects and assumed each laser oscillating in a single longitudinal mode with the same resonance frequency and the same pump current level. The effect of disorder in resonance frequencies will be briefly considered in Sec. IV. Mode coupling is rather generally non-Hermitian, i.e., it corresponds to $\kappa_{n,l} \neq \kappa^*_{l,n}$ for some index $n \neq l$. For dissipative coupling, i.e., if mode coupling is realized without amplifying elements, any eigenvalue of the matrix $\{\kappa_{n,l}\}$ has negative (for dissipative coupling) or vanishing (for conservative coupling) real part. Dissipative coupling arises rather generally when using diffractive coupling methods,[56,59,62,64,65,68,72,73,75] i.e., non-local coupling methods, such as those based on Talbot cavities[64,68,76] and diffractive optics. However, dissipative coupling can arise also via evanescent mode coupling, i.e., for local (nearest-neighbor) array coupling, in the presence of dissipative dielectrics, as discussed in Refs. 35 and 83–90. We note that a rather flexible method to tailor coupling constants $\kappa_{n,l}$ in a reconfigurable way has been suggested and experimentally demonstrated in a recent work.[75] In the following analysis, we will assume discrete rotational invariance along the ring so that the coupling matrix element $\kappa_{n,l}$ depends on the index difference $(l - n)$ solely, i.e.,

$$\kappa_{n,l} = \kappa_{l-n}. \tag{3}$$

For $l = n$, without loss of generality, the self-coupling term κ_0 can be assumed to be imaginary, i.e., $\kappa_0 = -i\gamma$ with $\gamma \geq 0$ for dissipative coupling: the term γ basically describes extra linear loss in each laser of the array arising from the coupling. Under such assumptions, the rate equations (1) and (2) take the form

$$\frac{dE_n}{dt} = (1 - i\alpha)Z_n E_n - \gamma E_n - i\sum_{\sigma \neq 0} \kappa_\sigma E_{n+\sigma}, \tag{4}$$

$$T\frac{dZ_n}{dt} = p - Z_n - (1 + 2Z_n)|E_n|^2, \tag{5}$$

with $\kappa_{-\sigma} = \kappa^*_\sigma$ and $\gamma = 0$ in the limiting case of Hermitian coupling. Equations (4) and (5) should be supplemented with the ring (periodic) boundary conditions

$$E_{n+N}(t) = E_n(t). \tag{6}$$

B. Stationary phase-locked laser supermodes

The laser equations (4) and (5) can display different types of stationary states and their dynamics depends largely on the coupling topology and the strength of coupling between the individual lasers. The simplest family of stationary states, corresponding to lasing states in the various supermodes of the ring, is given by[69,80]

$$E_n^{(st)}(t) = A\exp(iqn + i\omega t)\,, \quad Z_n^{(st)}(t) = Z, \tag{7}$$

where

$$Z = \gamma - \mathrm{Im}\left(\sum_{\sigma \neq 0} \kappa_\sigma \exp(iq\sigma)\right), \tag{8}$$

$$\omega = -\alpha Z - \mathrm{Re}\left(\sum_{\sigma\neq 0} \kappa_\sigma \exp(iq\sigma)\right), \tag{9}$$

$$A = \sqrt{\frac{p - Z}{1 + 2Z}}. \tag{10}$$

In the above equations, q is the Bloch wave number of the supermode, which is quantized and can assume N values according to the ring boundary conditions (6)

$$q = q_l = \frac{2\pi l}{N} \tag{11}$$

($l = 0, 1, 2, \ldots, N - 1$). Any supermode with a non-vanishing wave number q carries a topological charge given by[82] $T.C. = (1/2\pi)\sum_{n=1}^{N} E_n^* E_{n+1} = Nq/(2\pi)$. Note that, for a sufficiently large value of N, the Bloch wave number q can be basically considered a continuous variable, whereas for a small number of lasers in the ring, finite size effects should be properly considered; in particular, some differences occur for odd and even values of N.[69] In our work, we will typically assume a sufficiently large number N of lasers so that q can be treated as an almost continuous variable and do not consider distinctions between odd and even numbers of lasers. Note that the existence domain of the supermode with Bloch wave number q is defined by the inequality $p \geq Z$ so that the excess pump current thresholds of various Bloch supermodes are given by

$$p^{(th)}(q) = \gamma - \mathrm{Im}\left(\sum_{\sigma\neq 0} \kappa_\sigma \exp(iq\sigma)\right). \tag{12}$$

For a dissipative coupling, one has $p^{(th)}(q) \geq 0$. Note that in the limiting case of Hermitian coupling, i.e., for $\gamma = 0$ and $\kappa_{-\sigma} = \kappa_\sigma^*$, one has $p^{(th)}(q) = 0$ independent of q, i.e., all supermodes are degenerate in threshold. On the other hand, for non-Hermitian coupling, the threshold value of injection current depends on q, and a supermode with the lowest current threshold is rather generally found. We will specifically focus our analysis to three coupling configurations, corresponding to nearest-neighbor mode coupling.

1. Hermitian coupling

This coupling corresponds to $\kappa_\sigma = 0$ for $\sigma \neq \pm 1$ and $\kappa_{-1} = \kappa_1 \equiv \kappa$ real and positive. This case describes the ordinary Hermitian (conservative) mode coupling of nearest-neighbor lasers in the array, which was previously studied in Ref. 69. In this case, one has

$$Z = 0\,,\ \ \omega = -2\kappa\cos(q)\,,\ \ A = \sqrt{p}. \tag{13}$$

All supermodes have the same threshold value $p^{(th)} = 0$.

2. Type-I non-Hermitian coupling

This case corresponds to $\kappa_\sigma = 0$ for $\sigma \neq \pm 1$, $\kappa_{-1} = \kappa_1 = \kappa_R + i\kappa_I$ and $\gamma = 2\kappa_I$, where $\kappa_R > 0$ and $\kappa_I > 0$ describe conservative and dissipative couplings, respectively, between nearest neighbor lasers in the array. The Hermitian coupling is obtained in the limit $\kappa_I = 0$. This kind of non-Hermitian coupling is quite common in coupled laser arrays and has been considered in some previous studies,[84,85,90] especially for two coupled semiconductor lasers.[84,85] In this case, one has

$$Z = 2\kappa_I[1 - \cos(q)], \tag{14}$$

$$\omega = -2\alpha\kappa_I[1 - \cos(q)] - 2\kappa_R\cos(q), \tag{15}$$

$$A = \sqrt{\frac{p - 2\kappa_I[1 - \cos(q)]}{1 + 4\kappa_I[1 - \cos(q)]}}. \tag{16}$$

The threshold value of the various supermodes is given by

$$p^{(th)}(q) = 2\kappa_I[1 - \cos(q)]. \tag{17}$$

Note that the supermode with the lowest threshold $p^{(th)} = 0$ is the one with $q = 0$, i.e., with all lasers in the ring oscillating with the same phase.

3. Type-II non-Hermitian coupling

This case corresponds to $\kappa_\sigma = 0$ for $\sigma \neq \pm 1$, $\kappa_{-1} = \kappa \exp(-h)$, and $\kappa_1 = \kappa \exp(h)$, with κ and h real and positive. Note that the limiting case of Hermitian coupling is obtained for $h = 0$. This kind of non-Hermitian mode coupling has been recently introduced in Refs. 35, 49, 91, and 92 and non-Hermiticity arises here from the application of an imaginary gauge field (a complex Peierls' phase h) in the coupling constant κ. A possible physical implementation of an imaginary gauge field in coupled microring lasers, based on the use of anti-resonant link rings with dissipation, is discussed in Refs. 35, 49, and 92. For this coupling scheme, one has

$$Z = 2\kappa \sinh(h)[1 - \sin(q)], \tag{18}$$

$$\omega = -2\alpha\kappa \sinh(h)[1 - \sin(q)] - 2\kappa \cosh(h) \cos(q), \tag{19}$$

$$A = \sqrt{\frac{p - 2\kappa \sinh(h)[1 - \sin(q)]}{1 + 4\kappa \sinh(h)[1 - \sin(q)]}}. \tag{20}$$

The threshold value of the various supermodes is given by

$$p^{(th)}(q) = 2\kappa \sinh(h)[1 - \sin(q)]. \tag{21}$$

Note that the supermode with the lowest threshold $p^{(th)} = 0$ is the one with $q = \pi/2$. For such a supermode, the far-field emitted beam carries a non-vanishing orbital angular momentum, i.e., a topological charge, given by $T.C. = N/4$.[82] Note that the topological charge depends on the number N of lasers, while it is independent of the imaginary gauge field h.

The behavior of the excess pump current threshold curves $p^{(th)}$ and frequency ω of the laser array supermodes, versus the Bloch wave number q, for the three kinds of nearest-neighbor coupling schemes discussed above is shown in Fig. 1(c).

We note that type-I and type-II non-Hermitian couplings can be regarded as special cases of nearest-neighbor couplings with arbitrary (complex) values of κ_{-1}, κ_1, with $\kappa_{-1} \neq \kappa_1^*$. While the present analysis could be readily extended to include such a more general case, here we limit ourselves to consider type-I and type-II couplings, which are the more common types of nearest-neighbor couplings in lasers. Finally, it should be noted that in the case of global coupling other kinds of solutions to the laser equations (4)–(6) can be found, such as splay states and chimera states (i.e., coexisting synchronous and desynchronous oscillatory behavior).[80,93,94] Recently, chimera states in nearest-neighbor coupling semiconductor lasers with Hermitian coupling and frequency detuning have been studied in Ref. 79. However, in this work, we will not consider such types of solutions and their stability. While they are interesting from the viewpoint of complex dynamical systems and networks, in practical cases, one should avoid them and phase-locked states, with all lasers emitting in a synchronous way, are desired.

III. LINEAR STABILITY ANALYSIS

Dynamical instabilities in arrays of coupled semiconductor lasers are known to arise in a wide range of parameter operations corresponding to realistic conditions,[63,66,67,69,80] even when delayed coupling and frequency detuning effects are negligible. In particular, a detailed analysis of the instability arising in a ring geometry with nearest-neighbor Hermitian coupling has been presented by Li and Erneux in Ref. 69 (see also Ref. 80). A natural question then arises: what is the impact of non-Hermitian coupling on the onset of dynamical instabilities? Can non-Hermitian coupling help to prevent laser instabilities and force stable laser emission in the preferred supermode with $q = 0$ (all lasers in the array emitting in phase) or in a supermode that corresponds to a vortex beam in far-field? It is clear that some non-local coupling methods known in the literature, such as those based on the Talbot effect, can be regarded as a kind of non-Hermitian coupling scheme[95] and they help to achieve stable laser emission. To study the impact of non-Hermitian coupling on laser instabilities in a rather general framework, we performed a detailed linear stability analysis of the phase-locked solutions given by Eqs. (7)–(10), extending the analysis of Ref. 69 to account for a rather broad

class of non-Hermitian coupling configurations. As we will see, even for nearest-neighbor coupling non-Hermitian effects can effectively suppress the onset of dynamical instabilities and enable stable phase locking operation in a supermode with either $q = 0$ (for type-I non-Hermitian coupling) or $q = \pi/2$ (for type-II non-Hermitian coupling). After setting $E_n(t) = E_n^{(st)}(t)[1 + \delta E_n(t)]$ and $Z_n(t) = Z[1 + \delta Z_n(t)]$, the linearized equations that describe the evolution of small perturbations $\delta E_n(t)$ and δZ_n from the stationary state read as

$$\frac{d\delta E_n}{dt} = (1 - i\alpha)\delta Z_n - i\sum_{\sigma\neq 0}\kappa_\sigma \exp(iq\sigma)(\delta E_{n+\sigma} - \delta E_n), \tag{22}$$

$$T\frac{d\delta Z_n}{dt} = -(1 + 2A^2)\delta Z_n - A^2(1 + 2Z)(\delta E_n + \delta E_n^*), \tag{23}$$

with the periodic ring boundary conditions $\delta E_{n+N}(t) = \delta E_n(t)$. The most general solution to Eqs. (22) and (23) is a linear superposition of solutions of the form

$$\delta E_n(t) = R_1 \exp(iQn + \lambda t) + R_2^* \exp(-iQn + \lambda^* t), \tag{24}$$

$$\delta Z_n(t) = P \exp(iQn + \lambda t) + P^* \exp(-iQn + \lambda^* t), \tag{25}$$

where Q is the Bloch wave number of the perturbation [quantized like q according to Eq. (11)] and λ describes the growth rate of the perturbation. The complex amplitudes R_1, R_2, and P satisfy the homogeneous linear system

$$\lambda R_1 = (1 - i\alpha)P - i\theta_1 R_1, \tag{26}$$

$$\lambda R_2 = (1 + i\alpha)P + i\theta_2 R_2, \tag{27}$$

$$T\lambda P = -(1 + 2A^2)P - A^2(1 + 2Z)(R_1 + R_2), \tag{28}$$

where we have set

$$\theta_1 \equiv \sum_{\sigma\neq 0}\kappa_\sigma \exp(iq\sigma)[\exp(iQ\sigma) - 1], \tag{29}$$

$$\theta_2 \equiv \sum_{\sigma\neq 0}\kappa_\sigma^* \exp(-iq\sigma)[\exp(iQ\sigma) - 1]. \tag{30}$$

The growth rate λ is obtained from the corresponding eigenvalue problem, i.e., λ is a root of the cubic equation

$$\lambda^3 + c_1\lambda^2 + c_2\lambda + c_3 = 0, \tag{31}$$

where we have set

$$c_1 \equiv i(\theta_1 - \theta_2) + \frac{1 + 2A^2}{T}, \tag{32}$$

$$c_2 \equiv \theta_1\theta_2 + \frac{i(\theta_1 - \theta_2)(1 + 2A^2) + 2A^2(1 + 2Z)}{T}, \tag{33}$$

$$c_3 \equiv \frac{\theta_1\theta_2(1 + 2A^2)}{T} + \frac{A^2(1 + 2Z)[i(\theta_1 - \theta_2) - \alpha(\theta_1 + \theta_2)]}{T}. \tag{34}$$

Note that, for a given value of the Bloch wave number q of stationary array supermode, one has three possible values $\lambda = \lambda_l(Q)$ ($l = 1, 2, 3$) of the perturbation growth rate, which depend on the Bloch wave number Q of the perturbation. The stationary phase-locked supermode with Bloch wave number q, given by Eqs. (7)–(10), is thus linearly stable provided that the real part of any of the three eigenvalue $\lambda_l(Q)$ is positive or vanishing, for *any* wave number Q of the perturbation. Owing to phase invariance of the stationary state solution, one of the three eigenvalues vanishes at $Q = 0$. The roots of the cubic equation (31) are given in the most general case by Cardano′ formula; however, their form is rather cumbersome to be given here and in general one has to resort to a numerical computation of the eigenvalues and the corresponding domain of stability. Some analytical insights can be obtained under proper scaling of parameters, as suggested in Ref. 69. Taking into account that in a semiconductor laser T is a large parameter ($T \sim 100$–1000), we may introduce a small parameter

ϵ defined by $\epsilon = 1/\sqrt{T}$ and find the roots of Eq. (31) as a power series in ϵ. Moreover, since the instability arises for a strength of coupling constants of order $\sim\epsilon^2$,[69] we assume κ_σ small and of order $\sim\epsilon^2$, i.e., we set $\kappa_\sigma \equiv \epsilon^2\beta_\sigma$, with $\beta_\sigma \sim O(1)$. With such a scaling, one has $c_1 \sim \epsilon^2$, $c_2 \sim \epsilon^2$, and $c_3 \sim \epsilon^4$. We then look for a solution to the cubic equation (31) in power series of ϵ, namely, we assume

$$\lambda = \epsilon(\lambda_0 + \epsilon\lambda_1 + \cdots). \tag{35}$$

At leading order in ϵ, the three roots of the cubic equation are found to be given by

$$\lambda_1 = -\frac{c_3}{c_2} + o(\epsilon^2), \tag{36}$$

$$\lambda_{2,3} = \frac{c_3 - c_1c_2}{2c_2} \pm i\sqrt{c_2} + o(\epsilon^2), \tag{37}$$

with $c_1 = i(\theta_1 - \theta_2) + (1 + 2A^2)/T$, $c_2 \simeq 2A^2(1 + 2Z)/T$, and $c_3 \simeq (c_2/2)[i(\theta_1 - \theta_2) - \alpha(\theta_1 + \theta_2))]$. The stability condition, $\mathrm{Re}(\lambda_{1,2,3}) \le 0$, then yields

$$0 \le \mathrm{Re}(c_3) \le c_2\mathrm{Re}(c_1). \tag{38}$$

Substitution of Eqs. (32)–(34) into Eq. (38) and using Eqs. (29) and (30) finally yield the following stability conditions at leading order in ϵ:

$$\sum_{\sigma\neq 0}[1 - \cos(Q\sigma)][(\alpha - i)\kappa_\sigma \exp(iq\sigma) + c.c.] \ge 0, \tag{39}$$

$$\frac{1}{2}\sum_{\sigma\neq 0}[1 - \cos(Q\sigma)][(\alpha - i)\kappa_\sigma \exp(iq\sigma) + c.c.] \le \frac{1 + 2A^2}{T} - \sum_{\sigma\neq 0}[1 - \cos(Q\sigma)][i\kappa_\sigma \exp(iq\sigma) + c.c.], \tag{40}$$

which should be satisfied for any wave number $Q = 2\pi l/N$ ($l = 0, 1, 2, \ldots, N - 1$) of perturbation. The stability conditions (39) and (40) apply to a rather arbitrary coupling scheme, i.e., either local or global couplings, with the solely constraint of translational invariance. Let us now specialize the general results to the three local (nearest-neighbor) coupling schemes introduced in Sec. II [Fig. 1(c)].

A. Hermitian coupling

This case was considered in Ref. 69 and corresponds to $\kappa_\sigma = 0$ for $\sigma \neq \pm 1$ and $\kappa_1 = \kappa_{-1} = \kappa$ real and positive. In this case, conditions (39) and (40) read explicitly as

$$\cos(q) \ge 0, \tag{41}$$

$$\kappa \le \frac{1 + 2p}{2\alpha T\cos(q)[1 - \cos(Q)]}, \tag{42}$$

which have been previously derived in Ref. 69. Equation (41) indicates that only the supermodes with Bloch wave number q in the range $|q| < \pi/2$ are stable states, whereas Eq. (42) shows that a Hopf instability at the frequency $\omega_H = \sqrt{c_2} = \sqrt{2p/T}$ arises for large enough coupling constant κ [violation of Eq. (42) corresponds to the two complex-conjugate eigenvalues $\lambda_{2,3}$, given by Eq. (37), to become unstable]. The Hopf bifurcation frequency ω_H corresponds to the free-running relaxation oscillation frequency.[51] Clearly, the most unstable perturbation for the emergence of the Hopf instability is the one with Bloch wave number $Q = \pi$ and the maximum value of coupling constant, below which the phase-locked supermode with wave number q remains stable, is given by

$$\kappa^{(\max)} = \frac{1 + 2p}{4\alpha T\cos(q)}. \tag{43}$$

Note that the most unstable supermode is the one with $q = 0$, i.e., the supermode with in-phase laser emission, as previously shown in Ref. 69.

B. Type-I non-Hermitian coupling

Let us assume $\kappa_{-1} = \kappa_1 \equiv \kappa_R + i\kappa_I$, where $\kappa_R > 0$ and $\kappa_I > 0$ are the conservative and dissipative couplings, respectively, and $\kappa_\sigma = 0$ for $|\sigma| > 1$. In this case, the stability conditions (39) and (40) read explicitly as

$$(\kappa_R \alpha + \kappa_I)\cos(q) \geq 0, \tag{44}$$

$$\kappa_R \alpha - \kappa_I \leq \frac{1 + 2A^2}{2T\cos(q)[1 - \cos(Q)]}. \tag{45}$$

Like in the Hermitian case discussed above, Eq. (44) shows that the supermodes with $\cos(q) < 0$ are always unstable, while stable supermodes necessarily should correspond to a Bloch wave number q with $\cos(q) \geq 0$. The main impact of non-Hermitian coupling is clear when considering the stability condition (45). Remarkably, for a sufficiently large value of the dissipative coupling term as compared to the conservative one, namely, for

$$\kappa_I \geq \alpha \kappa_R. \tag{46}$$

Equation (45) is satisfied for $\cos(q) > 0$, regardless of the strength of the couplings κ_I and κ_R. This means that, provided that Eq. (46) is satisfied, non-Hermitian coupling can prevent the onset of the Hopf instability observed in the Hermitian limit as the coupling strength between neighboring lasers is increased.

C. Type-II non-Hermitian coupling

Let us assume $\kappa_{-1} = \kappa \exp(-h)$ and $\kappa_1 = \kappa \exp(h)$, with κ and h real and positive constant, and $\kappa_\sigma = 0$ for $|\sigma| > 1$. In this case, the stability conditions (39) and (40) read explicitly as

$$\alpha \cosh(h)\cos(q) + \sinh(h)\sin(q) > 0, \tag{47}$$

$$\kappa[\alpha \cosh(h)\cos(q) - \sinh(h)\sin(q)] < \frac{1 + 2A^2}{2T[1 - \cos(Q)]}. \tag{48}$$

Note that, in this case, the supermode with the lowest current threshold, corresponding to $q = \pi/2$, is always stable, regardless of the strength κ of the laser coupling, even for a small value of the non-Hermitian gauge field h. Therefore type-II non-Hermitian coupling is expected to be a suitable and robust means to generate stable phase-locked laser emission in a supermode carrying a non-vanishing topological charge. The supermode with $q = \pi/2$ carries a topological charge $T.C. = N/4$,[82] which is independent of the imaginary gauge field h. The fact that for type-II non-Hermitian coupling the lowest threshold supermode carries a non-vanishing orbital angular momentum that stems from the asymmetric coupling $\kappa_{-1} \neq \kappa_1$, which introduces a chiral behavior in the dynamics[30,31] and a preferred *directional* transport along the chain of coupled lasers:[35] the non-Hermitian gauge field h *reduces* the stability domain of the in-phase supermode $q = 0$, while it favors oscillation of the $q = \pi/2$ supermode.

The approximate stability conditions, given by Eqs. (39) and (40) and obtained by an asymptotic form of the roots of the cubic determinantal equation, correctly capture the main role played by non-Hermitian coupling in preventing or enhancing the onset of the Hopf instability. As an example, Fig. 2 shows the exact numerically computed stability domains of the in-phase supermode state ($q = 0$) for type-I non-Hermitian coupling in the (κ_R, κ_I) plane, and for type-II non-Hermitian coupling in the (κ, h) plane. The exact stability domains are also compared to those obtained by the asymptotic analysis of the eigenvalues of the cubic determinantal equation. Note that, as expected, the asymptotic analysis provides a good approximation of the stability boundaries only for relatively small values of coupling strength. Note also that, as excepted from the asymptotic analysis, while type-I non-Hermitian coupling prevents the onset of instability for the in-phase supermode $q = 0$ [Fig. 2(a)], type-II non-Hermitian coupling narrows the stability region of this supermode [Fig. 2(b)].

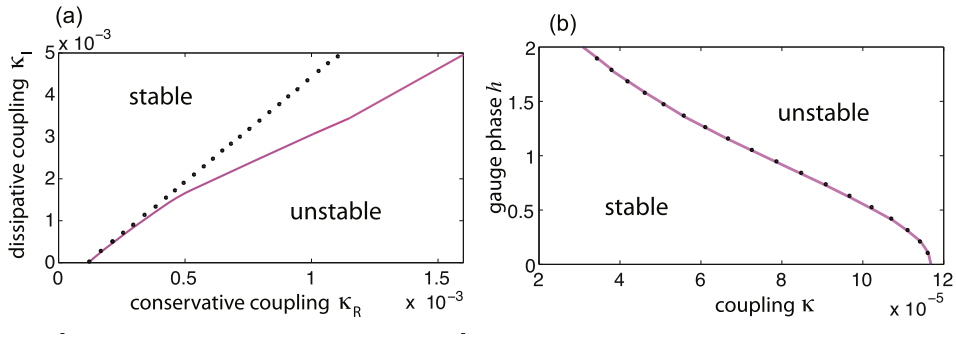

FIG. 2. Numerically computed stability diagram of the in-phase supermode state ($q = 0$) (a) for type-I non-Hermitian coupling ($\kappa_{-1} = \kappa_1 = \kappa_R + i\kappa_I$) in the plane ($\kappa_R$, κ_I) of conservative/dissipative coupling strengths and (b) for type-II non-Hermitian coupling ($\kappa_{-1} = \kappa \exp(-h)$, $\kappa_1 = \kappa \exp(h)$) in the ($\kappa$, h) plane. Parameter values are $\alpha = 5$, $T = 600$, and $p = 0.2$. Dotted curves refer to the stability boundaries as obtained from the asymptotic analysis of the roots of the cubic determinantal equation (31). The Hermitian limit is retrieved for $\kappa_I = 0$ in (a) and $h = 0$ in (b). In this case, the Hopf instability arises for a coupling strength larger than $\kappa^{(\max)} \simeq 1.167 \times 10^{-4}$, given by Eq. (43) with $q = 0$.

IV. NUMERICAL RESULTS

The ability of non-Hermitian couplings to prevent the onset of dynamical instabilities and to force stable laser oscillation in the in-phase ($q = 0$) supermode or in a chiral ($q = \pi/2$) supermode has been checked by direct numerical simulations of laser rate equations (1) and (2). Parameter values used in the simulations are typical of semiconductor laser arrays and comparable to those used in previous theoretical studies:[63,67,69,70] $\alpha = 5$, $T = 600$, and p ranging from 0.003 to 0.2. The rate equations have been numerically solved using an accurate variable-step Runge-Kutta method, assuming $N = 8$ lasers in the ring. As an initial condition, we typically assumed small random values of amplitudes E_n for the electric fields and the stationary values $Z_n = p$ of excess carrier densities in each laser of the array. After initial relaxation, oscillation transient describing laser switch on, different dynamical regimes can be observed, which depend on parameter values but can also depend on initial conditions, i.e., different runs starting from small random noise can result in different dynamical behaviors. This is a clear signature of multi-stability and of highly nonlinear dynamics of laser array systems, which is very common in coupled nonlinear oscillator models (see for instance Refs. 96–98 and references therein). Multi-stability clearly arises from the fact that many supermodes (7) can be stable in the same domain of parameter space. In addition, other attractors such as periodic or quasi-periodic limit cycles and chaotic attractors might exist as well. If the domains of attraction of some stable states are intertwined, the output of the system is unpredictable, and even a small noise can cause the system to hop freely among the many coexisting stable attractors (see, for instance, Refs. 96 and 97). Despite multi-stability, here we show that, under appropriate choice of non-Hermitian parameters, the basin of attraction of the stable supermode with the lowest laser threshold can basically cover most of small-amplitude random-phase initial conditions so that after transient switch on the laser most likely emits in a stable supermode. Hence our design method provides a robust route for stable high-power laser array design. As an example, Fig. 3(a) shows a typical behavior of laser emission started from initial random noise as obtained for nearest-neighbor Hermitian coupling in the Hopf instability region for a pump parameter $p = 0.2$ and for a coupling constant $\kappa = 2 \times 10^{-4}$, which is ~1.71 times larger than the maximum value $\kappa^{(\max)} \simeq 1.167 \times 10^{-4}$ predicted by the linear stability analysis [Eq. (43) and Fig. 2]. The laser amplitudes undergo self-pulsation as a result of the Hopf instability, at a frequency $\omega_H \simeq 243$ which is very close to the theoretical value $\omega_H = \sqrt{2p/T}$ predicted by the linear stability analysis. For Hermitian coupling, more irregular behaviors are observed as the coupling strength κ is further increased, as shown for example in Fig. 3(b). The suppression of supermode instability for type-I non-Hermitian coupling is shown in Fig. 4(a). Parameter values are as in Fig. 3(a), except that the couplings $\kappa_1 = \kappa_2 = \kappa_R + i\kappa_I$ have a non-vanishing dissipative part κ_I. Note that, for $\kappa_I = \alpha\kappa_R$ chosen in the numerical simulations, according to the linear stability analysis [Eq. (46)] all supermodes of the array are locally stable. Since $q = 0$ is the supermode with the lowest pump current threshold, it is the most rapidly growing mode from initial noise, and thus this supermode is expected to have the

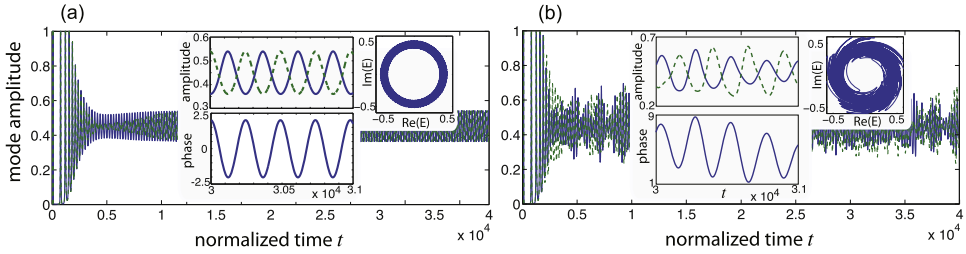

FIG. 3. Numerically computed laser switch on dynamics in a ring array made of $N = 8$ lasers for nearest-neighbor Hermitian coupling in the oscillatory (Hopf) instability regime. Parameter values are $T = 600$, $p = 0.2$, $\alpha = 5$, and $\kappa = 2 \times 10^{-4}$ in (a), $\kappa = 1.5 \times 10^{-3}$ in (b). An initial condition is a small random noise of the field amplitudes E_n, and stationary values $Z_n = p$ of normalized excess carriers. The figure shows the behavior of modal amplitude $|E_n|$ for the two modes $n = 1$ (solid curve) and $n = 4$ (dashed curve) of the array. Insets: upper left inset shows the detailed behavior of the mode amplitudes after relaxation oscillation transient; lower left inset shows the behavior of the phase difference between the two modes; right inset depicts the phase space evolution of field amplitude [R$e(E)$, I$m(E)$] of the $n = 1$ laser in the array, after initial relaxation oscillation transient.

wider basin of attraction. An example of transient laser switch on, leading to stable oscillation in the $q = 0$ supermode, is shown in Fig. 4(a). A statistical analysis of laser switch on dynamics has been performed by considering 200 different initial conditions, corresponding to the same small amplitude $|E_l(0)| = 1 \times 10^{-7}$ of the electric field in each laser but different phase distributions, randomly taken with uniform distribution in the range $(0, 2\pi)$. In all cases, after initial transient, the attractor of the dynamics is one of the supermodes given by Eq. (7), with the supermode $q = 0$ being the most probable outcome (~66% probability), i.e., with the largest basin of attraction. The other observed attractors are the two higher threshold supermodes with wave numbers $q = \pm 2\pi/N_d = \pm\pi/4$, which are found with ~17% probability each of them. In no case have oscillatory nor irregular behaviors been observed for such a ratio of κ_I/κ_R and pump level. By slightly increasing the ratio κ_I/κ_R, from α to 1.5α, the basin of attraction of the $q = 0$ supermode widens, and in 200 runs, the probability that the laser emits in the $q = 0$ supermode increases from ≃66% up to ≃99%. It should be noted that the phase space of the laser system may not be covered by the domains of attraction of stable phase-locked states, and other attractors such as periodic or quasi-periodic limit cycles and chaotic attractors may exist—each one with its own basin of attraction. Therefore, even though all phase-locked supermodes are stable, for some parameter values the initial condition can be located in the domain of attraction of a more complex attractor. This is shown, for example, in Fig. 4(b), where a large coupling constant κ_R is assumed, yet keeping the ratio $\kappa_I/\kappa_R = \alpha$ at the same values as in Fig. 4(a). In this case, to achieve stable phase-locking emission in the $q = 0$ supermode, one can either decrease the pump current level p or increase the ratio κ_I/κ_R of dissipative to conservative coupling terms, which broadens the basin of attraction of the $q = 0$ supermode thus avoiding irregular laser output. For example, by increasing the ratio κ_I/κ_R from α to 4α [Fig. 4(c)], stable oscillation in the $q = 0$ supermode is observed in 99.5% cases of runs after transient laser switch on.

For type-II non-Hermitian coupling, stable laser oscillation is expected to occur on the lowest-threshold $q = \pi/2$ supermode, resulting in a far-field vortex beam carrying orbital angular momentum. Figure 5(a) shows an example of stable emission in the $q = \pi/2$ supermode at a relatively low pump current level. Like for type-I non-Hermitian coupling, the vortex-beam emission is not always the

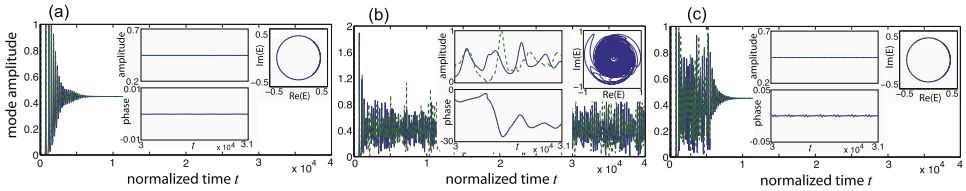

FIG. 4. Laser switch on dynamics for type-I non-Hermitian coupling. (a) $\kappa_R = 2 \times 10^{-4}$ and $\kappa_I = \alpha\kappa_R$, (b) $\kappa_R = 1.5 \times 10^{-3}$ and $\kappa_I = \alpha\kappa_R$, and (c) $\kappa_R = 1.5 \times 10^{-3}$ and $\kappa_I = 4\alpha\kappa_R$. Other parameter values are as in Fig. 3 ($T = 600$, $p = 0.2$, $\alpha = 5$).

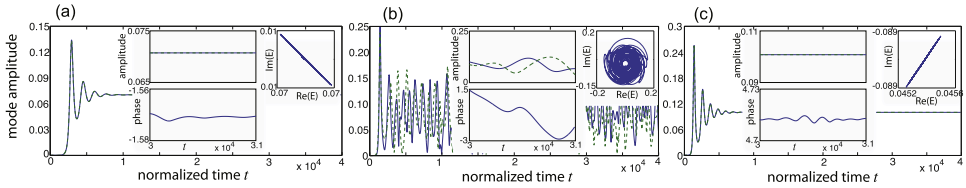

FIG. 5. Laser switch on dynamics for type-II non-Hermitian coupling. Parameter values are (a) $\kappa = 2 \times 10^{-4}$, $h = 3$, $p = 0.005$; (b) $\kappa = 2 \times 10^{-4}$, $h = 3$, $p = 0.01$; (c) $\kappa = 2 \times 10^{-4}$, $h = 4$, $p = 0.01$. Other parameter values are as in Fig. 3 ($\alpha = 5$, $T = 600$). Stable phase-locking laser emission in the $q = \pi/2$ supermode is observed in (a) and (c). In 200 runs with small-amplitude random phase initial conditions, in (a) and (c), the probability for the laser to emit in the $q = \pi/2$ supermode is $\simeq$74% and 100%, respectively.

most likely attractor of the dynamics when the coupling strength κ and/or the pump current level p are increased. Indeed, irregular emission can be observed as well [see Fig. 5(b)]. Nevertheless, by increasing the non-Hermitian parameter h, the basin of attraction of the $q = \pi/2$ supermode widens, and one can restore stable emission of the vortex supermode. This is shown, as example, in Fig. 5(c).

In the previous examples, we assumed that all the lasers oscillate on a single longitudinal mode with the same resonance frequency. However, in practice, the lasers can show slight deviations of their resonance frequencies from the ideal one, e.g., due to imperfections in fabrication. While deviations of the resonance frequencies much smaller than mode coupling can be neglected, they can destroy phase locking when become comparable to the strength of mode coupling. In the case of Hermitian coupling, for a large number N of lasers disorder in the resonance frequencies makes the array supermodes localized rather than extended (because of the Anderson localization) so that independent oscillations in clusters of lasers are observed (see, e.g., the recent experiment[99]). For gradient frequency detunings in the array, complex patterns such as chimera states have been predicted to arise for Hermitian coupling in Ref. 79.

The Anderson localization arising from disorder in the resonance frequencies of the lasers occurs as well as for complex but symmetry coupling, i.e., for type-I non-Hermitian coupling. Interestingly, type-II non-Hermitian coupling, corresponding to asymmetric mode-coupling, provides robust chiral

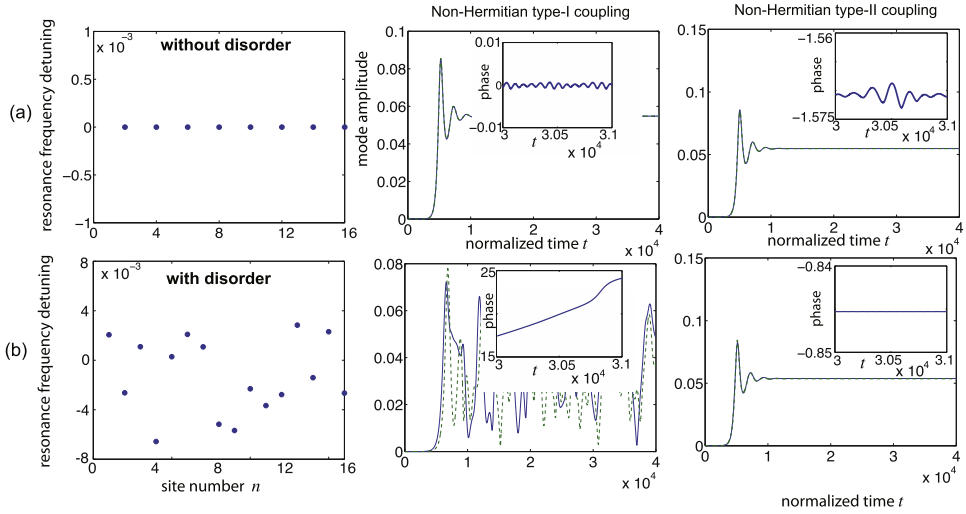

FIG. 6. Laser switch on dynamics for type-I (middle column) and type-II (right column) non-Hermitian couplings in the presence of disorder of laser resonance frequencies for a ring array of $N = 16$ coupled lasers. The distribution of the resonance frequency detuning (in units of $1/\tau_p$) is shown in the left column. In (a), there is not disorder, whereas in (b) disorder of resonance frequencies is considered of strength comparable to the coupling constant. In the central and right panels of (a) and (b), solid and dashed curves refer to the field in lasers at sites $n = 1$ and $n = 8$ of the ring. The insets show the behavior of the phase difference of the fields in the two rings. Parameter values are $\alpha = 5$, $T = 600$, $p = 0.003$, and $\kappa_1 = \kappa_2 = 0.002 + 0.01i$ for type-I coupling (central column), $\kappa_1 = 3.66 \times 10^{-6}$, $\kappa_2 = 0.0109$ for type-II coupling (right column).

transport along the ring, which is immune to moderate disorder strength owing to the phenomenon of non-Hermitian delocalization transition[100] (see also Refs. 35, 91, and 101): the supermode with the lost threshold $q = \pi/2$ is not localized by moderate disorder of resonance frequencies in the ring. Therefore, we expect that type-II non-Hermitian coupling, besides of combating dynamical instabilities, can ensure stable laser emission even in the presence of moderate strength of disorder in the laser resonance frequencies. As an example, Fig. 6 compares laser dynamics for type-I and type-II non-Hermitian coupling with the same disorder of the resonance frequencies of the lasers in the ring. Parameter values are the same in the two cases, with comparable strength of mode coupling such that, without disorder, both coupling methods ensure stable phase-locked oscillation [Fig. 6(a)]. In the presence of moderate disorder, in type-I non-Hermitian coupling, stable oscillation is typically destroyed, with the appearance of irregular oscillations [Fig. 6(b), middle panel]. On the other hand, for type-II non-Hermitian coupling, stable phase-locked laser emission persists despite of disorder [Fig. 6(b), right panel].

V. CONCLUSIONS

In this work, we have considered the long-standing problem of forcing stable supermode emission in laser arrays in the perspective of the emerging field of non-Hermitian photonics.[1,2,4] Even when time delay effects are negligible, semiconductor laser arrays are known to undergo a great variety of dynamical behaviors, ranging from self-pulsing to chaos, and to show complex spatiotemporal patterns such as chimera states.[63,66,67,69,79,80,93] While complexity of laser array behavior can be of interest from the viewpoint of the physics of complex systems, combating the onset of dynamical instabilities and forcing synchronous laser emission is desirable in most photonic applications. Using a standard rate equation model describing the dynamics of semiconductor laser arrays on a ring,[69] we have shown rather generally that non-Hermitian coupling engineering of laser arrays is able to mitigate the onset of dynamical instability and can force laser emission in a stable supermode. Traditional methods of laser phase locking based on global couplings, such as diffractive coupling in Talbot cavities, can be regarded as a kind of non-Hermitian coupling engineering. Here we have shown that non-Hermitian coupling can effectively stabilize laser emission in a given supermode using local (nearest-neighbor) non-Hermitian coupling schemes. In particular, we considered two kinds of non-Hermitian local couplings, referred to as type-I and type-II non-Hermitian couplings. In the former case, all the lasers oscillate with the same phase; whereas in the latter case, $\pi/2$ phase slips between adjacent lasers can be realized, resulting in a far-field vortex beam emission carrying orbital angular momentum. As compared to type-I non-Hermitian coupling, type-II non-Hermitian coupling realizes a chiral transport along the ring which is robust against moderate disorder of resonance frequencies. Our results show that the emerging field of non-Hermitian photonics can find important application into a rather old problem of laser science and technology and are expected to stimulate further theoretical and experimental studies. In particular, type-II non-Hermitian coupling provides a promising scheme in laser array design for combating the detrimental effects of laser instabilities as well as unavoidable disorder of resonance frequencies due to fabrication imperfections.

ACKNOWLEDGMENTS

S.L. acknowledges useful discussions with D. Gomila, I. Fischer, Y. Kominis, and V. Kovanis. Hospitality at the IFISC (CSIC-UIB), Palma de Mallorca is also gratefully acknowledged.

[1] L. Feng, R. El-Ganainy, and L. Ge, "Non-Hermitian photonics based on parity-time symmetry," Nat. Photonoics **11**, 752 (2017).
[2] R. El-Ganainy, K. G. Makris, M. Khajavikhan, Z. H. Musslimani, S. Rotter, and D. N. Christodoulides, "Non-Hermitian physics and PT-symmetry," Nat. Phys. **14**, 11 (2018).
[3] V. V. Konotop, J. Yang, and D. A. Zezyulin, "Nonlinear waves in PT-symmetric systems," Rev. Mod. Phys. **88**, 035002 (2016).
[4] S. Longhi, "Parity-time symmetry meets photonics: A new twist in non-Hermitian optics," Europhys. Lett. **120**, 64001 (2017).
[5] H. Zhao and L. Feng, "Parity-time symmetric photonics," Nat. Sci. Rev. **5**, 183 (2018).
[6] C. M. Bender and S. Boettcher, "Real spectra in non-Hermitian Hamiltonians having PT symmetry," Phys. Rev. Lett. **80**, 5243 (1998).

[7] C. M. Bender, "Making sense of non-Hermitian Hamiltonians," Rep. Prog. Phys. **70**, 947 (2007).
[8] M. V. Berry, "Physics of non-Hermitian degeneracies," Czech. J. Phys. **54**, 1039 (2004).
[9] N. Moiseyev, *Non-Hermitian Quantum Mechanics* (Cambridge University Press, 2011).
[10] A. Ruschhaupt, F. Delgado, and J. G. Muga, "Physical realization of PT-symmetric potential scattering in a planar slab waveguide," J. Phys. A **38**, L171 (2005).
[11] R. El-Ganainy, K. G. Makris, D. N. Christodoulides, and Z. H. Musslimani, "Theory of coupled optical PT-symmetric structures," Opt. Lett. **32**, 2632 (2007).
[12] K. G. Makris, R. El-Ganainy, D. N. Christodoulides, and Z. H. Musslimani, "Beam dynamics in PT symmetric optical lattices," Phys. Rev. Lett. **100**, 103904 (2008).
[13] A. Guo, G. J. Salamo, D. Duchesne, R. Morandotti, M. Volatier-Ravat, V. Aimez, G. A. Siviloglou, and D. N. Christodoulides, "Observation of PT-symmetry breaking in complex optical potentials," Phys. Rev. Lett. **103**, 093902 (2009).
[14] S. Longhi, "Quantum-optical analogies using photonic structures," Laser Photonics Rev. **3**, 243 (2009).
[15] C. E. Rüter, K. G. Makris, R. El-Ganainy, D. N. Christodoulides, M. Segev, and D. Kip, "Observation of parity-time symmetry in optics," Nat. Phys. **6**, 192 (2010).
[16] S. Longhi, "Optical realization of relativistic non-Hermitian quantum mechanics," Phys. Rev. Lett. **105**, 013903 (2010).
[17] A. Szameit, M. C. Rechtsman, O. Bahat-Treidel, and M. Segev, "PT-symmetry in honeycomb photonic lattices," Phys. Rev. A **84**, 021806(R) (2011).
[18] A. Regensburger, C. Bersch, M.-A. Miri, G. Onishchukov, D. N. Christodoulides, and U. Peschel, "Parity-time synthetic photonic lattices," Nature **488**, 167 (2012).
[19] S. Longhi, "PT-symmetric laser absorber," Phys. Rev. A **82**, 031801 (2010).
[20] Y. D. Chong, L. Ge, and A. D. Stone, "PT-symmetry breaking and laser-absorber modes in optical scattering systems," Phys. Rev. Lett. **106**, 093902 (2011).
[21] S. Longhi, "Coherent perfect absorption in a homogeneously broadened two-level medium," Phys. Rev. A **83**, 055804 (2011).
[22] S. Longhi, "Bloch oscillations in complex crystals with PT symmetry," Phys. Rev. Lett. **103**, 123601 (2009).
[23] Z. Lin, H. Ramezani, T. Eichelkraut, T. Kottos, H. Cao, and D. N. Christodoulides, "Unidirectional invisibility induced by PT-symmetric periodic structures," Phys. Rev. Lett. **106**, 213901 (2011).
[24] S. Longhi, "Invisibility in PT-symmetric complex crystals," J. Phys. A: Math. Theor. **44**, 485302 (2011).
[25] L. Feng, Y.-L. Xu, W. S. Fegadolli, M.-H. Lu, J. E. Oliveira, V. R. Almeida, Y.-F. Chen, and A. Scherer, "Experimental demonstration of a unidirectional reflectionless parity-time metamaterial at optical frequencies," Nat. Mater. **12**, 108 (2013).
[26] A. Mostafazadeh, "Invisibility and PT symmetry," Phys. Rev. A **87**, 012103 (2013).
[27] B. Peng, S. K. Özdemir, F. Lei, F. Monifi, M. Gianfreda, G. L. Long, S. Fan, F. Nori, C. M. Bender, and L. Yang, "Parity-time-symmetric whispering-gallery microcavities," Nat. Phys. **10**, 394 (2014).
[28] H. Hodaei, M.-A. Miri, M. Heinrich, D. N. Christodoulides, and M. Khajavikhan, "Parity-time-symmetric microring lasers," Science **346**, 975 (2014).
[29] L. Feng, Z. J. Wong, R.-M. Ma, Y. Wang, and X. Zhang, "Single-mode laser by parity-time symmetry breaking," Science **346**, 972 (2014).
[30] S. Longhi and L. Feng, "PT-symmetric microring laser-absorber," Opt. Lett. **39**, 5026 (2014).
[31] B. Peng, S. K. Özdemir, M. Liertzer, W. Chen, J. Kramer, H. Yilmaz, J. Wiersig, S. Rotter, and L. Yang, "Chiral modes and directional lasing at exceptional points," Proc. Natl. Acad. Sci. U. S. A. **113**, 6845 (2016).
[32] P. Miao, Z. Zhang, J. Sun, W. Walasik, S. Longhi, N. M. Litchinitser, and L. Feng, "Orbital angular momentum microlaser," Science **353**, 464 (2016).
[33] S. Longhi and L. Feng, "Unidirectional lasing in semiconductor microring lasers at an exceptional point," Photonics Res. **5**, B1 (2017).
[34] Z. J. Wong, Y. L. Xu, J. Kim, K. O'Brien, Y. Wang, L. Feng, and X. Zhang, "Lasing and anti-lasing in a single cavity," Nat. Photonics **10**, 796 (2016).
[35] S. Longhi, D. Gatti, and G. Della Valle, "Robust light transport in non- Hermitian photonic lattices," Sci. Rep. **5**, 13376 (2015).
[36] A. U. Hassan, H. Hodaei, M.-A. Miri, M. Khajavikhan, and D. N. Christodoulides, "Nonlinear reversal of the PT-symmetric phase transition in a system of coupled semiconductor microring resonators," Phys. Rev. A **92**, 063807 (2015).
[37] H. Hodaei, M. A. Miri, A. U. Hassan, W. Hayenga, M. Heinrich, D. N. Christodoulides, and M. Khajavikhan, "Parity-time-symmetric coupled microring lasers operating around an exceptional point," Opt. Lett. **40**, 4955 (2015).
[38] M. H. Teimourpour, L. Ge, D. N. Christodoulides, and R. El-Ganainy, "Non-Hermitian engineering of single mode two dimensional laser arrays," Sci. Rep. **6**, 33253 (2016).
[39] H. Hodaei, M.-A. Miri, A. U. Hassan, W. E. Hayenga, M. Heinrich, D. N. Christodoulides, and M. Khajavikhan, "Single mode lasing in transversely multi-moded PT-symmetric microring resonators," Laser Photonics Rev. **10**, 494 (2016).
[40] A. U. Hassan, B. Zhen, M. Soljacic, M. Khajavikhan, and D. N. Christodoulides, "Dynamically encircling exceptional points: Exact evolution and polarization state conversion," Phys. Rev. Lett. **118**, 093002 (2017).
[41] J. Wiersig, "Enhancing the sensitivity of frequency and energy splitting detection by using exceptional points: Application to microcavity sensors for single particle detection," Phys. Rev. Lett. **112**, 203901 (2014).
[42] Z.-P. Liu, J. Zhang, S. K. Özdemir, B. Peng, H. Jing, X.-Y. Lu, C.-W. Li, L. Yang, F. Nori, and Y.-X. Liu, "Metrology with $\mathcal{PT}$-symmetric cavities: Enhanced sensitivity near the $\mathcal{PT}$-phase transition," Phys. Rev. Lett. **117**, 110802 (2016).
[43] W. Chen, S. K. Ozdemir, G. Zhao, J. Wiersig, and L. Yang, "Exceptional points enhance sensing in an optical microcavity," Nature **548**, 192 (2017).
[44] H. Hodaei, A. U. Hassan, S. Wittek, H. Garcia-Gracia, R. El-Ganainy, D. N. Christodoulides, and M. Khajavikhan, "Enhanced sensitivity at higher-order exceptional points," Nature **548**, 187 (2017).
[45] Z. Gao, S. T. M. Fryslie, B. J. Thompson, P. S. Carney, and K. D. Choquette, "Parity-time symmetry in coherently coupled vertical cavity laser arrays," Optica **4**, 323 (2017).

[46] Y. Kominis, V. Kovanis, and T. Bountis, "Spectral signatures of exceptional points and bifurcations in the fundamental active photonic dimer," Phys. Rev. A **96**, 053837 (2017).
[47] H. Zhao, P. Miao, M. H. Teimourpour, S. Malzard, R. El-Ganainy, H. Schomerus, and L. Feng, "Topological Hybrid silicon microlasers," Nat. Commun. **9**, 981 (2018).
[48] M. Parto, S. Wittek, H. Hodaei, G. Harari, M. A. Bandres, J. Ren, M. C. Rechtsman, M. Segev, D. N. Christodoulides, and M. Khajavikhan, "Complex edge-state phase tansitions in 1D topological laser arrays," Phys. Rev. Lett. **120**, 113901 (2018).
[49] S. Longhi, "Non-Hermitian gauged topological laser arrays," Ann. Phys., e-print arXiv:1801.00996.
[50] M. Pan, H. Zhao, P. Miao, S. Longhi, and L. Feng, "Photonic zero mode in a non-Hermitian photonic lattice," Nat. Commun. **9**, 1308 (2018).
[51] T. Erneux and P. Glorieux, *Laser Dynamics* (Cambridge University Press, 2010).
[52] C. O. Weiss and R. Vilaseca, *Dynamics of Lasers* (Wiley-VCH, Weinheim, Germany, 1991).
[53] A. C. Newell and J. V. Moloney, *Nonlinear Optics* (Addison-Wesley, New York, 1992).
[54] S. Longhi, "$\mathcal{PT}$ symmetric mode-locking," Opt. Lett. **41**, 4518 (2016).
[55] *Diode Laser Arrays*, edited by D. Botez and D. R. Scifres (Cambridge University Press, 1994).
[56] A. F. Glova, "Phase locking of optically coupled lasers," Quantum Electron. **33**, 283 (2003).
[57] T. Y. Fan, "Laser beam combining for high-power, high-radiance sources," IEEE J. Sel. Top. Quantum Electron. **11**, 567 (2005).
[58] M. C. Soriano, J. Garca-Ojalvo, C. R. Mirasso, and I. Fischer, "Complex photonics: Dynamics and applications of delay-coupled semiconductors lasers," Rev. Mod. Phys. **85**, 421 (2013).
[59] J. Katz, S. Margalit, and A. Yariv, "Diffraction coupled phase-locked semiconductor laser array," Appl. Phys. Lett. **42**, 554 (1983).
[60] E. Kapon, J. Katz, and A. Yariv, "Supermode analysis of phase-locked arrays of semiconductor lasers," Opt. Lett. **10**, 125 (1984).
[61] C. P. Lindsey, E. Kapon, J. Katz, S. Margalit, and A. Yariv, "Single contact tailored gain phased array of semiconductor lasers," Appl. Phys. Lett. **45**, 722 (1984).
[62] J. R. Leger, M. L. Scott, and W. B. Veldkamp, "Coherent addition of AlGaAs lasers using microlenses and diffractive coupling," Appl. Phys. Lett. **52**, 1771 (1988).
[63] H. G. Winful and S. S. Wang, "Stability of phase locking in coupled semiconductor laser arrays," Appl. Phys. Lett. **53**, 1894 (1988).
[64] J. R. Leger, "Lateral mode control of an AlGaAs laser array in a Talbot cavity," Appl. Phys. Lett. **55**, 334 (1989).
[65] L. Liu, "Lau cavity and phase locking of laser arrays," Opt. Lett. **14**, 1312 (1989).
[66] K. Otsuka, "Self-induced phase turbulence and chaotic itinerancy in coupled laser systems," Phys. Rev. Lett. **65**, 329 (1990).
[67] H. G. Winful and L. Rahman, "Synchronized chaos and spatiotemporal chaos in arrays of coupled lasers," Phys. Rev. Lett. **65**, 1575 (1990).
[68] D. Mehuys, W. Streifer, R. G. Waarts, and D. F. Welch, "Modal analysis of linear Talbot-cavity semiconductor lasers," Opt. Lett. **16**, 823 (1991).
[69] R. D. Li and T. Erneux, "Preferential instability in arrays of coupled lasers," Phys. Rev. A **46**, 4252 (1992).
[70] A. Hohl, A. Gavrielides, T. Erneux, and V. Kovanis, "Localized synchronization in two coupled nonidentical semiconductor lasers," Phys. Rev. Lett. **78**, 4745 (1997).
[71] J. Xu, S. Li, K. K. Lee, and Y. C. Chen, "Phase locking in a two-element laser array: A test of the coupled-oscillator model," Opt. Lett. **18**, 513 (1993).
[72] J. R. Terry, K. S. Thornburg, D. J. DeShazer, G. D. VanWiggeren, S. Zhu, P. Ashwin, and R. Roy, "Synchronization of chaos in an array of three lasers," Phys. Rev. E **59**, 4036 (1999).
[73] F. Rogister, K. S. Thornburg, L. Fabiny, M. Möller, and R. Roy, "Power-law spatial correlations in arrays of locally coupled lasers," Phys. Rev. Lett. **92**, 093905 (2004).
[74] S. Yanchuk, A. Stefanski, T. Kapitaniak, and J. Wojewoda, "Dynamics of an array of mutually coupled semiconductor lasers," Phys. Rev. E **73**, 016209 (2006).
[75] D. Brunner and I. Fischer, "Reconfigurable semiconductor laser networks based on diffractive coupling," Opt. Lett. **40**, 3854 (2015).
[76] L. Wang, J. Zhang, Z. Jia, Y. Zhao, C. Liu, Y. Liu, S. Zhai, Z. Ning, X. Xu, and F. Liu, "Phase-locked array of quantum cascade lasers with an integrated Talbot cavity," Opt. Express **24**, 30275 (2016).
[77] Y. Kominis, V. Kovanis, and T. Bountis, "Controllable asymmetric phase-locked states of the fundamental active photonic dimer," Phys. Rev. A **96**, 043836 (2017).
[78] V. Pal, C. Tradonsky, R. Chriki, A. A. Friesem, and N. Davidson, "Observing dissipative topological defects with coupled lasers," Phys. Rev. Lett. **119**, 013902 (2017).
[79] J. Shena, J. Hizanidis, V. Kovanis, and G. P. Tsironis, "Turbulent chimeras in large semiconductor laser arrays," Sci. Rep. **7**, 42116 (2017).
[80] M. Silber, L. Fabiny, and K. Wiesenfeld, "Stability results-for in-phase and splay-phase states of solid-state laser arrays," J. Opt. Soc. Am. B **10**, 1121 (1993).
[81] M. Nixon, M. Fridman, E. Ronen, A. A. Friesem, N. Davidson, and I. Kanter, "Controlling synchronization in large laser networks using number theory," Phys. Rev. Lett. **108**, 214101 (2012).
[82] V. Pal, C. Trandonsky, R. Chriki, G. Barach, A. A. Friesem, and N. Davidson, "Phase locking of even and odd number of lasers on a ring geometry: Effects of topological-charge," Opt. Express **23**, 13041 (2015).
[83] H. A. Haus, H. Statz, and I. W. Smith, "Frequency locking of modes in a ring laser," IEEE J. Quantum Electron. **21**, 78 (1985).
[84] H. G. Winful, S. Allen, and L. Rahman, "Validity of the coupled-oscillator model for laser-array dynamics," Opt. Lett. **18**, 1810 (1993).

[85] A. Scirè, C. J. Tessone, and P. Colet, "Dynamics of coupled self-pulsating semiconductor lasers," IEEE J. Quantum Electron. **41**, 272 (2005).
[86] M. Greenberg and M. Orenstein, "Irreversible coupling by use of dissipative optics," Opt. Lett. **29**, 451 (2004).
[87] N. V. Alexeeva, I. V. Barashenkov, K. Rayanov, and S. Flach, "Actively coupled optical waveguides," Phys. Rev. A **89**, 013848 (2014).
[88] J. Xu and Y. Chen, "General coupled mode theory in non-Hermitian waveguides," Opt. Express **23**, 22619 (2015).
[89] S. Longhi, "Non-Hermitian tight-binding network engineering," Phys. Rev. A **93**, 022102 (2016).
[90] D. E. Hill, "Phased array tracking of semiconductor laser arrays with complex coupling coefficients," IEEE J. Sel. Top. Quantum Electron. **23**, 1501209 (2017).
[91] S. Longhi, D. Gatti, and G. Della Valle, "Non-Hermitian transparency and one-way transport in low-dimensional lattices by an imaginary gauge field," Phys. Rev. B **92**, 094204 (2015).
[92] D. Leykam, K. Y. Bliokh, C. Huang, Y. D. Chong, and F. Nori, "Edge modes, degeneracies, and topological numbers in non-Hermitian systems," Phys. Rev. Lett. **118**, 040401 (2017).
[93] W.-J. Rappel, "Dynamics of a globally coupled laser model," Phys. Rev. A **49**, 2750 (1994).
[94] J. Singha and N. Gupte, "Spatial splay states and splay chimera states in coupled map lattices," Phys. Rev. E **94**, 052204 (2016).
[95] For laser arrays with diffraction coupling in a Talbot cavity, the form of the non-Hermitian coupling matrix $\{\kappa_{n,l}\}$ is given in Ref. 68. See also Ref. 72.
[96] K. Wiesenfeld and P. Hadley, "Attractor crowding in oscillator arrays," Phys. Rev. Lett. **62**, 1335 (1989).
[97] V. Kovanis, A. Gavrielides, and J. A. C. Gallas, "Labyrinth bifurcations in optically injected diode lasers," Eur. Phys. J. D **58**, 181 (2010).
[98] W. L. Ku, M. Girvan, and E. Otto, "Dynamical transitions in large systems of mean field-coupled Landau-Stuart oscillators: Extensive chaos and cluster states," Chaos **25**, 123122 (2015).
[99] M. A. Bandres, S. Wittek, G. Harari, M. Parto, J. Ren, M. Segev, D. N. Christodoulides, and M. Khajavikhan, "Topological insulator laser: Experiment," Science **359**, eaar4005 (2018).
[100] H. A. Hatano and Nelson, "Localization transitions in non-Hermitian quantum mechanics," Phys. Rev. Lett. **77**, 570 (1996).
[101] Z. Gong, Y. Ashida, K. Kawabata, K. Takasan, S. Higashikawa, and M. Ueda, "Topological phases of non-Hermitian systems," e-print arXiv:1802.07964v1 (2018).